Cytometry 19:27–41 (1995).

Quantitative Analysis of Comparative Genomic Hybridization

Stanislas du Manoir, Evelin Schröck, Martin Bentz, Michael R. Speicher, Stefan Joos, Thomas Ried, Peter Lichter, and Thomas Cremer

Abteilung Organisation komplexer Genome, Deutsches Krebsforschungszentrum, Im Neuenheimer Feld 280 (S.d.M., M.B., S.J., P.L.), and Institut für Humangenetik, Im Neuenheimer Feld 328 (E.S., M.R.S., T.R., T.C.), 69120 Heidelberg, Germany

Received for publication April 5, 1994; accepted July 8, 1994

Comparative genomic hybridization (CGH) is a new molecular cytogenetic method for the detection of chromosomal imbalances. Following cohybridization of DNA prepared from a sample to be studied and control DNA to normal metaphase spreads, probes are detected via different fluorochromes. The ratio of the test and control fluorescence intensities along a chromosome reflects the relative copy number of segments of a chromosome in the test genome. Quantitative evaluation of CGH experiments is required for the determination of low copy changes, e.g., monosomy or trisomy, and for the definition of the breakpoints involved in unbalanced rearrangements. In this study, a program for quantitation of CGH preparations is presented. This program is based on the extraction of the fluorescence ratio profile along each chromosome, followed by averaging of individual profiles from several meta phase spreads. Objective parameters critical for quantitative evaluations were tested, and the criteria for selection of suitable CGH preparations are described. The granularity of the chromosome painting and the regional inhomogeneity of fluorescence intensities in metaphase spreads proved to be crucial parameters. The coefficient of variation of the ratio value for chromosomes in balanced state (CVBS) provides a general quality criterion for CGH experiments. Different cutoff levels (thresholds) of average fluorescence ratio values were compared for their specificity and sensitivity with regard to the detection of chromosomal imbalances. © 1995 Wiley-Liss, Inc.

Key terms: Comparative genomic hybridization, CGH, fluorescence in situ hybridization, chromosomal imbalances, tumor cytogenetics, quantitative image analysis, fluorescence ratio imaging

Comparative genomic hybridization (CGH; 8) is a new molecular cytogenetic approach based on two-color fluorescence in situ suppression hybridization (3,8,10). CGH allows a comprehensive analysis of gains and losses of entire chromosomes as well as mapping of the chromosomal subregions present in unbalanced copy numbers. Chromosomal imbalances can be detected by CGH only if they are present in a high proportion of the test sample cells. Test DNA isolated from the tissue sample of interest, e.g., from a tumor, and control DNA isolated from diploid cells (46,XX or 46,XY) are labeled separately with different reporter molecules. Equal amounts of test and control genomic DNA are mixed and hybridized to normal metaphase chromosome preparations together with an excess of unlabeled Cot1 fraction of human DNA. After the detection of the hybridized sequences with two fluorochromes, e.g., fluorescein isothiocyanate (FITC) for the tumor DNA and tetrarhodamine isothiocyanate (TRITC) for the normal control DNA, the ratios of the fluorescence intensities are measured along individual chromosomes. From these ratios, the balanced state, or over-, or under-representation of a given chromosome or chromosome segment in the test cell sample can be deduced.

It should be noted that CGH reveals only relative copy number changes. The absolute number of a given chromosome segment present in the majority of test cells cannot be deduced solely by this method. Ratios of comparative hybridization signals for diploid, triploid, etc. cells cannot be distinguished from each other.

The potential of this method to determine the chro-

Parts of this work were presented at an AMCA Workshop, Amsterdam, June 25–26, 1993, and at the topical Workshop "CGH Imaging," Edinburgh, June 3–4, 1994, sponsored by the EC Concerted Action "Automation Molecular Cytogenetic Analyses" (CA-AMCA project BIOMED-1 CT921307).

This work was supported in part by grants from the European Community (GENO-CT91-0029, SSMA, T.C.; GENO-91003, S.d.M.), the Sander Stiftung (T.C.), and the Thyssen-Stiftung (P.L.).

Address reprint requests to S. du Manoir, National Center for Human Genome Research, NIH, Building 49, Room 4b24, 9000 Rockville Pike, Bethesda, MD 20892.

mosomal map positions of multiple genetic imbalances in solid tumors has been demonstrated in several studies (3,7–10,19,20,22–24). The detection of chromosome aberrations in tumors by cytogenetic banding techniques is often very difficult due to poor banding quality or insufficient spreading of the metaphase chromosomes. In contrast, CGH has a distinct advantage, in that the extent of genetic imbalances can be mapped on reference metaphase chromosomes. Genomic DNA is the only material required from the test cell specimen. Such DNA can also be prepared from archived tumor specimens that are formalin fixed and paraffin embedded (22).

In many instances, gross genetic imbalances in tumor genomes such as high-level DNA amplifications are readily detectable after CGH by eye using conventional fluorescence microscopy. However, a quantitation of fluorescence intensity based on digital image analysis is required for an accurate CGH analysis of low copy number changes, particularly if they are not present in the vast majority of cells. Furthermore, digital fluorescence analysis is necessary for the assessment of multiple DNA gains and losses. In this study, we describe a method useful for such a quantitative evaluation. The procedure is based on the extraction of fluorescence ratio profiles along individual chromosomes. In a second step, average fluorescence ratio profiles are calculated from homologous chromosomes of several metaphase spreads (22). The program described in this study was used to analyze some 140 tumor cases in two laboratories. Crucial steps to obtain a reliable evaluation include; 1) definition of objective parameters to select CGH preparations suitable for quantitative evaluation, 2) standardization of image acquisition, 3) chromosome segmentation, 4) fluorescence background estimation, 5) determination of the central value providing a balanced representation of a given chromosome segment, and 6) definition of thresholds for unbalanced segments present in lower or higher copy number. The sensitivity and specificity of the CGH evaluation procedure was tested for differently defined thresholds using various tumor specimens. CGH data were compared with results obtained by cytogenetic banding analysis as well as by interphase cytogenetic analysis.

MATERIALS AND METHODS

CGH Experiments

Comparative genomic hybridization was carried out as described elsewhere (3,19,20).

Program for CGH Evaluation. The program was developed on the basis of an image analysis package (TCL-software; Multihouse, Amsterdam, The Netherlands) implemented on a MacIntosh Quadra 950. User interaction is limited to the selection of a single chromosome in each reference metaphase spread for the correction of the optical shift, chromosome identification based on 4,6-diamidino-2-phenylindole dihydrochloride (DAPI) banding, and the elimination of chromosomes with incorrect chromosomal axes (see below). For a given batch of images, the interactive procedures (steps 2 and 4) are carried out consecutively on each image. Thereafter, the batch of images is processed automatically. The program comprises the following steps in sequential order: 1) image acquisition; 2) correction of the optical shift; 3) determination of the chromosome axis; 4) chromosome identification; 5) determination of the FITC, TRITC, and DAPI-profiles; 6) averaging of individual profiles; 7) determination of the thresholds; and 8) presentation of the results.

Image acquisition. The 512 × 512 pixels gray-level images were acquired using a cooled charge-coupled device (CCD) camera (Photometrics, Tucson, AZ) equipped with a Kodak KAF 1,400 chip (sampling 0.108 pixel/μm). The camera was mounted on an Zeiss Axiophot microscope equipped for epifluorescence. CGH images were acquired using a ×63 objective (Plan Neofluar, N.A.1.25). FITC, TRITC, and DAPI images of each reference metaphase spread were recorded. The fluorophores were selectively imaged using the following filter sets: FITC-fluorescence, Filter No. 10 (BP 450–490, FT 510, BP 515-565); TRITC-fluorescence, Filter No. 15 (BP 546, FT 580, LP 590); DAPI-fluorescence, BP 365, FT 395, BP 450–490. A 100 W mercury lamp was precisely adjusted by overlapping the focused lamp image with the lamp mirror image. A homogeneous illumination of the optical field was obtained by changing the collector position according to defined homogeneity criteria (Fig. 1). Images larger than 512 × 512 pixels (for the magnification used here) suffered from nonhomogeneous illumination. Image contrast was increased by closing the field diaphragm to the border of the image acquisition area; this resulted in a field diameter of approximately 90 μm in the object plane. Exposure times were chosen for each fluorochrome in order to obtain maximum chromosomal pixels values that equal one-half of the dynamic range of the camera (12 bits/2 = 4,096/2). Twelve-bit images were converted to 8-bit images according to the maximum pixel value of the image. All optical settings as well as the exposure times were kept constant for the images recorded from a series of metaphase spreads acquired for a single case. The exposure times in the present experiments were in the range of 4–6 s for FITC and 3–5 s for TRITC (Fig. 2). Optimal exposure times (2–5 s) for DAPI were also important, since DAPI images were used both for chromosome identification and the formation of segmentation masks (see below). The relatively short exposure times required to take these images indicate that the demands for the CCD camera do not include the integration of very weak signals. The test DNA was generally visualized using FITC. TRITC was used for the control DNA. The same results were obtained in some cases with a reversed painting scheme (data not shown). In this publication, FITC always refers to the detection of tumor DNA, while TRITC refers to control DNA.

Correction of optical shift. When filter cubes are moved to collect the fluorescence emission of a single fluorochrome, optical and mechanical imperfections may cause image shifts relative to each other. These shifts were corrected by the alignment of the gravity center of

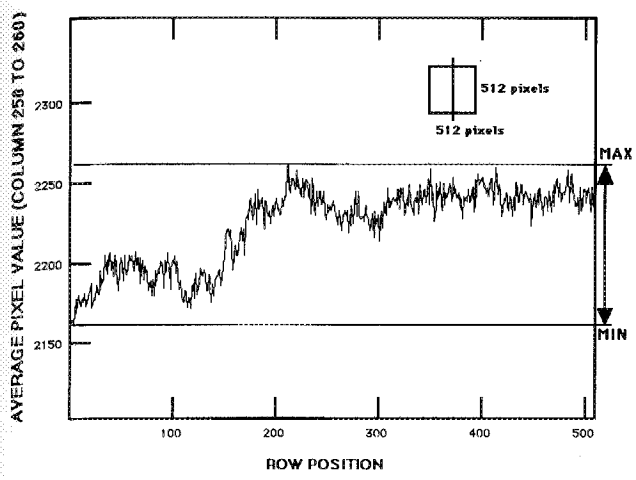

FIG. 1. Homogeneity of the illumination. Images (512 × 512 pixels) of an empty field on a slide used for comparative genomic hybridization (CGH) experiments were acquired using a 12-bit cooled charge-coupled device (CCD) camera (Photometrics) with an exposure time of 10 s and the 4,6-diamidino-2-phenylindole dihydrochloride (DAPI) filter combination. The **inset** (top right) shows the line that was drawn to mark the area of measurement. The average pixel intensity for ten columns (each covering 512 rows) is presented as a function of the position. The illumination field is considered homogeneous if values above 0.1 are obtained using the following formula: (maximum pixel intensity value − minimum pixel intensity value)/minimum pixel intensity. In the presented case, the value is 0.05.

a single chromosome in the FITC, TRITC, and DAPI images (modified from 26). Iterating segmentation was applied in order to obtain a segmentation mask of approximately the same area in the three images. This segmentation was used only for the correction of the optical shift. Mask gravity centers were computed as well as contours of the mask. After an initial alignment, the final alignment was performed by moving the second image by one pixel in the eight directions of Freeman; the final position corresponds to the minimal integrated gray value in the first image through the border line (contour) of the chromosome mask (after binary dilatation) in the second image.

Determination of chromosome axis. Automatic chromosome segmentation for further measurements was achieved on the DAPI image after 1) zeroing the pixel values with gray level less than 30 (scale 256; gray levels less than 30 correspond to background pixels that are remote from chromosomes using the current mode to choose the exposure time) and 2) applying a "Hat" convolution (13 × 13 pixels; see 21). The mode of the gray-level histogram of the Hat filtered DAPI image was used as the threshold. This resulted in satisfactory chromosome segmentation masks even of the short arms of the acrocentric chromosomes (Fig. 3). These masks were used 1) to calculate a FITC by TRITC pixel-by-pixel ratio image for each metaphase as described previously (3) and 2) as a basis for the determination of chromosome axes. The Hilditch skeletons (5) were calculated for each chromosome after 1) filling of the holes inside in the chromosome masks that did not exceed 300 pixels and 2) calculating the convex hull of the mask. Branching points in skeletons are attributable to 1) failure to obtain separate chromosome masks from attaching or overlapping chromosomes by the segmentation process and 2) the separation of the sister chromatids of one chromosome. For chromosome skeletons containing branching points, the segmentation process was repeated without user interaction using two different thresholds (for overlapping chromosomes or split chromatids). The final chromosome axis (Fig. 4) was obtained after extension of the chromosomal skeleton tips and smoothing (modified from 18). No interactive correction of chromosome axes was made.

Chromosome identification. The fluorescence banding pattern obtained after DAPI staining was used for chromosome identification (Fig. 2d). Chromosome identification was facilitated by using the DAPIinverse video image resembling a Giemsa banding. User interaction included the notation of the chromosome number and the chromosome orientation. The chromosome axes were displayed, and chromosomes with incorrect axes were excluded from evaluation. Commonly, due to overlapping chromosomes or incorrect axis, zero to five chromosomes per metaphase spread were excluded from analysis.

Determination of FITC, TRITC, and DAPI profiles. Gray-level segmented images were obtained by assigning zero values for pixels that were not inside the chromosome masks created by the segmentation process. The profiles for the FITC, TRITC, and DAPI gray-level segmented images were computed by sampling perpendicular to the chromosome axis using bilinear interpolation (Fig. 5b). The chromosome ends were defined on the basis of the DAPI and the TRITC intensities. The chromosome profiles were enlarged by linear interpolation to a predefined size for each chromosome type according to chromosome length measurements (17). For example, the length of chromosome 3 was set to 153 pixels (Fig. 5c). The FITC and TRITC fluorescence background values were estimated as the average gray value of the whole corresponding initial image excluding any areas containing interphase nuclei. In a pilot study, the above definition of background was superior to other definitions based on the nonchromosomal (and nuclear) area of the images (see Discussion). The fluorescence ratio profile was calculated as the quotient of FITC and TRITC intensities after background subtraction (Fig. 5d).

Averaging of individual profiles. The mode value of the histogram of the fluorescence ratio profile of all individual chromosomes of each metaphase was normalized to one (Fig. 5d,e). The normalization was necessary to compensate for eventual scale shifts due to the conversion of the 12-bit to 8-bit images. After this normalization, the arithmetic mean of the profile values of each chromosome type was computed (Fig. 5f).

Determination of thresholds. In cases where information on tumor ploidy was not available, a balanced state of chromosomes was defined by the central value,

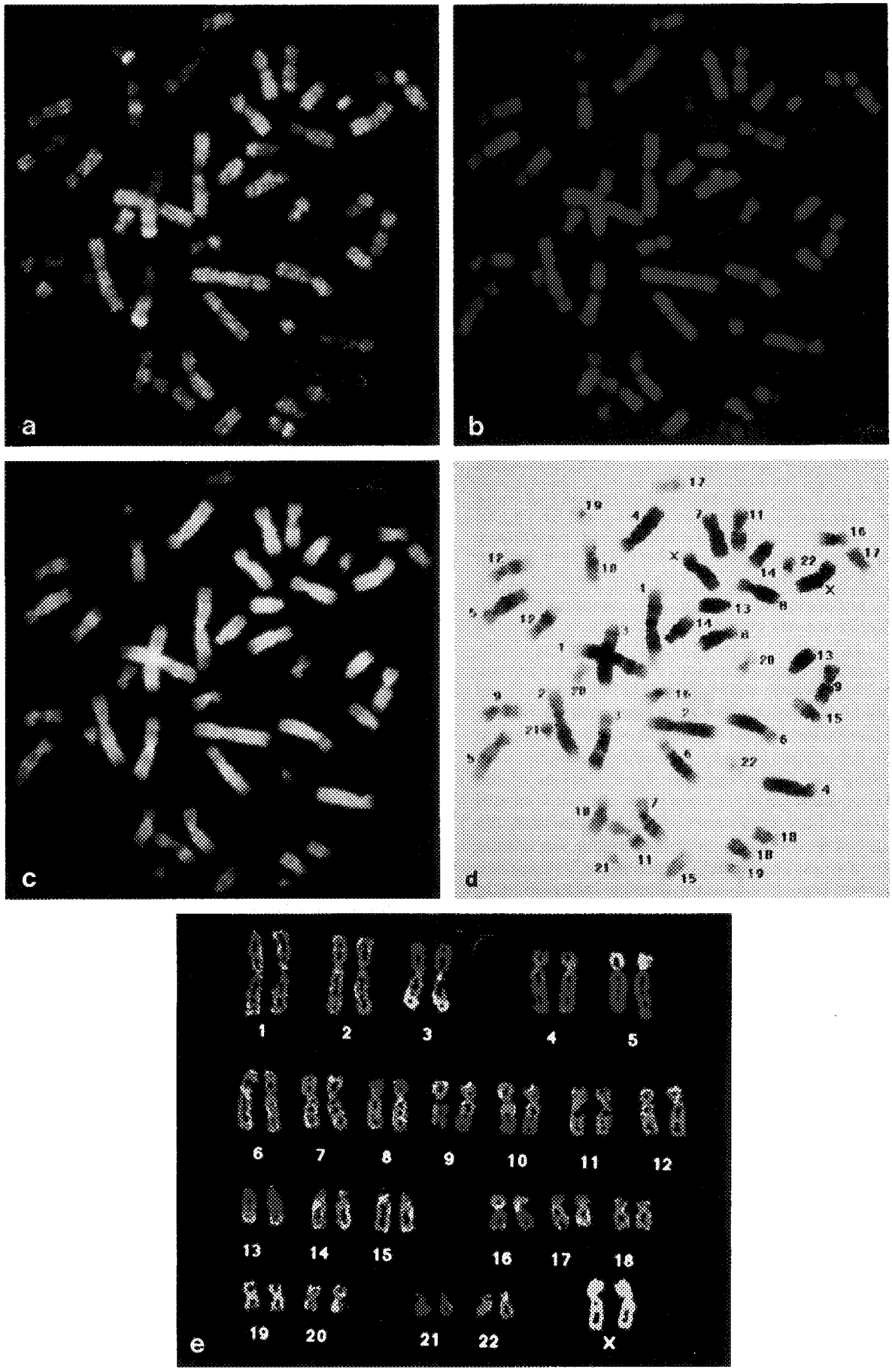

FIG. 2.

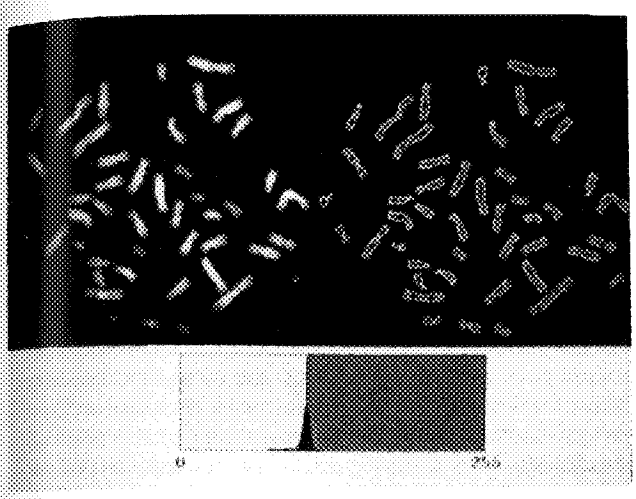

FIG. 3. Segmentation masks of a metaphase spread. **Left:** DAPI image. **Right:** Gray-level image after segmentation. **Bottom:** The mode of the gray-value histogram of the DAPI image (Hat filtered) is used as threshold for segmentation.

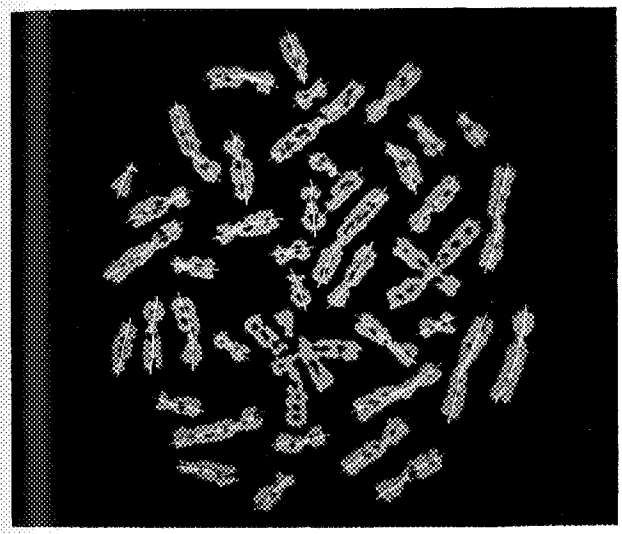

FIG. 4. Determination of the chromosomal axes on the segmentation masks of a metaphase spread. Chromosomal axes were derived from the skeletonization of the segmentation masks followed by an elongation of the skeletons beyond the segmentation masks.

FIG. 2. CGH experiments using DNA extracted from a primary small-cell lung carcinoma (SCLC). Images of a normal metaphase spread (46,XX; **a**) hybridized with SCLC DNA subsequently detected with fluorescein isothiocyanate (FITC; **b**) hybridized with control DNA (46,XY) subsequently detected with tetrarhodamine isothiocyanate (TRITC) and (**c**) counterstained with DAPI. **d:** Identification of the chromosome on the basis of an inverse video DAPI image. **e:** Fluorescence ratio image (see Materials and Methods and ref. 3) of the same metaphase. The chromosomes were interactively ordered to facilitate the comparison of chromosome homologues. A three-color look-up table was chosen for the visualization of the pixel-by-pixel FITC/TRITC ratio. Chromosome areas displayed in green represent high ratio values corresponding to gains in the tumor; red areas represent low ratio values and indicate losses in the tumor. Blue corresponds to a balanced state of the chromosome material.

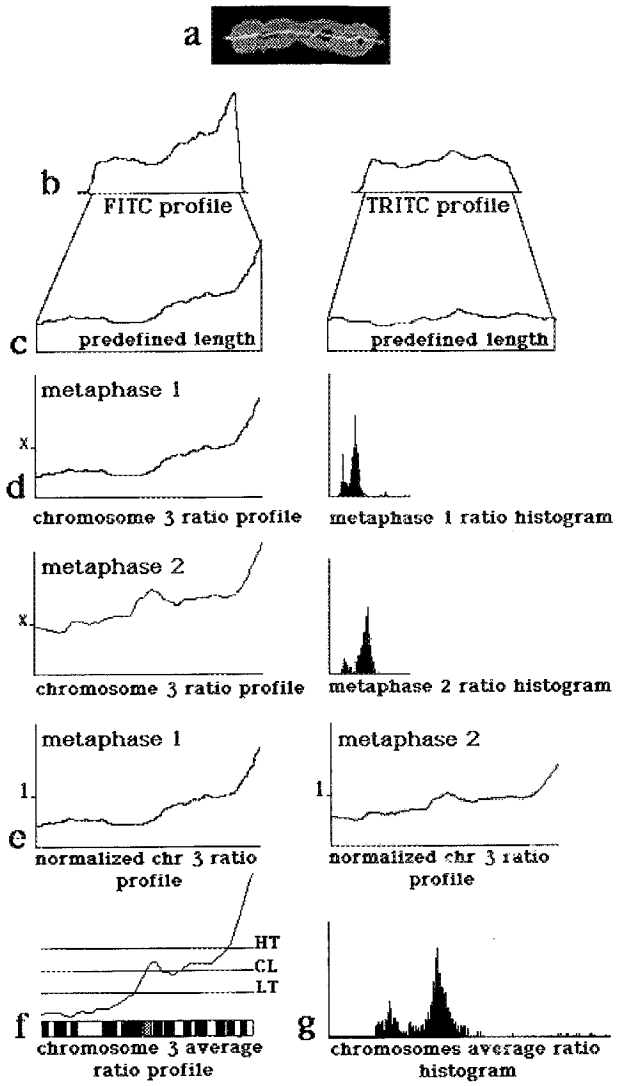

FIG. 5. Schematic representation of the steps used for the quantitation of CGH experiments. **a:** Chromosomal axis on the segmentation mask of a chromosome 3. **b:** FITC and TRITC profiles are extracted by calculating the mean of the pixel values located in lines perpendicular to the chromosomal axis inside of the segmentation mask. **c:** Profiles are linearly stretched to a predefined size. **d:** After background subtraction, FITC-to-TRITC ratio profiles are computed. **e:** Fluorescence-ratio profiles are normalized using the mode of the ratio-value histogram for each metaphase (see d). **f:** Average ratio profiles are obtained by averaging the individual profiles. This is displayed along the ISCN chromosome idiogram. The central line (CL) representing the balanced state is defined as the mode of the histogram of the average ratio profile for all chromosome types (**g**). The normal range is defined as the interval between the lower (LT) and the higher threshold (HT; 50% thresholds displayed).

i.e., the mode of the histogram of the resulting average profile values for all chromosomes (Fig. 5f,g). This value reflects the most abundant fluorescence ratio observed and does not necessarily correspond to the presence of two copies, i.e., a diploid state (Fig. 5g). In triploid or tetraploid cells, for example, this value corresponds to chromosomes present in three and four copies, respectively.

Depending on the availability of information on the ploidy of a test sample, three categories were defined to calculate both the central value (balanced state) and the thresholds for chromosomes present in unbalanced copy numbers: The first category comprised cases without information on the ploidy level. In routine tumor samples used for CGH, for example, the ploidy level was generally not known. In the second category, ploidy was estimated by interphase cytogenetics of tumor nuclei using DNA probes that map to chromosome segments with fluorescence ratios indicating a balanced state (see below). The third category reflects cases in which the ploidy was known from DNA-index measurements, e.g., by flow or image cytometry. The calculations for the determination of the assumed thresholds indicating gains or losses are described for each of these categories in the following.

1. Determination of thresholds for average ratio profiles without any DNA ploidy information: Thresholds were arbitrarily defined as the theoretical value that would be expected in a diploid tumor cell population for a trisomy or a monosomy of a certain chromosome in 50% of the test cells (i.e., 1.25 for a trisomy and 0.75 for a monosomy). The sensitivity of such thresholds decreased with increasing ploidy levels of the test cell population.

2. Determination of thresholds with an approximation of the DNA ploidy based on interphase cytogenetics: Analysis of the copy number of a chromosomal region in nuclei of the test sample could be performed by fluorescence in situ hybridization (FISH) using region-specific probes. The average number of interphase signals (per nucleus) for a region presenting a ratio value close to the central line (balanced state) provided the basis for the estimation of the ploidy. The closest round integer to the average number of interphase signals was assumed to provide the ploidy level. The multiplicative coefficients of the central value were calculated using the following formula: lower threshold = (ploidy level − 0.5)/ploidy level; upper threshold = (ploidy level + 0.5)/ploidy level. This resulted in values of 0.75 and 1.25 for diploid or pseudodiploid tumor cells, 0.83 and 1.17 for pseudotriploid, 0.88 and 1.12 for pseudotetraploid tumor cells, and so forth.

3. Determination of threshold values in cases with DNA content measurements: The mean of the average fluorescence ratio values obtained for homologous chromosomes from a series of metaphase spreads was proportional to the DNA index of the cell population. Consequently, instead of using the mode (see above) in this particular case, the central value was calculated as the mean of the average fluorescence ratio. To calculate the multiplicative coefficients of the central value, the following formula was used: lower threshold = (DNA index − 0.5)/DNA index; upper threshold = (DNA index + 0.5)/DNA index. Accordingly, when the DNA index is available, the absolute copy number of chromosomes could be estimated from fluorescence ratio values assuming that fluorescence measurements are performed within the linear range.

Alternatively, a statistical threshold can be defined on the basis of the distribution of the ratio value of balanced chromosomes (see below under Variability of Ratio Profiles).

Presentation of results. Average ratio profiles are displayed at the right side of chromosome idiograms (ISCN 1985, 400 bands; 6). The central line reflects the balanced state, whereas the lower and upper thresholds are represented by the lines left and right of the central line, respectively (Fig. 5f). Furthermore, the program provides a set of parameters describing the quality of the CGH experiments, including the number of chromosome homologues used in the analysis, the mean fluorescence ratios, the length of the chromosomes, the fluorescence background staining, and the granularity of the painting (for definition of the latter, see below under Quality Controls). In order to display the summary of a series of CGH experiments of a particular tumor entity, gains and losses of chromosome material are visualized as bars next to chromosome idiograms (see, e.g., 19,20).

Quality controls. The following parameters and criteria are used to select reference metaphase spreads and to judge the usefulness of images taken from CGH preparations for quantitative assessment. Selection is performed both during the image acquisition step and during image processing. Usually, ten-well spread metaphases fitting entirely into the 512 × 512 pixel frame were imaged for each case. Seventy to one hundred percent of these metaphase spreads fulfilled the selection criteria for the image analysis. All the images of the tumor cases analyzed by CGH in our two laboratories were stored and were used to assess the range of variation of the parameters.

CGH preparations. The following parameters are considered to be most important in obtaining CGH preparations useful for quantitation. 1) Equal concentration of the control and test DNA should be used. 2) Only metaphases with optimal spreading, i.e., zero or very few overlapping chromosomes, should be selected for image analysis. 3) Immunological background staining should be minimal. It is particularly critical in this respect to avoid residual cytoplasm in metaphase spreads. 4) Sometimes, an entire batch of metaphase spread preparations appears to be unsuitable due to a speckled chromosome painting pattern. CGH experiments using a mixture of differently labeled normal genomic DNA is, therefore, applied to test each batch of metaphase spread preparations. 5) The choice of proper control DNA is also important. DNA extracted from the peripheral blood of one of our donors resulted in fluorescence ratios for chromosome 19 that were systematically beyond the normal range. This phenomenon was overcome by using control DNA isolated from another donor. 6) Metaphase spreads selected for the analysis of a given case should provide a similar degree of chromosome condensation. In our experiments, the mean length of chromosome 1 for each case was in the range of 8–14 μm.

Suppression in situ hybridization. The measurement of fluorescence ratios meaningful for the detection

of chromosome copy number changes critically depends on efficient suppression of interspersed, repetitive sequences present in the test and control genomic DNA. Suppression is achieved by the addition of nonlabeled Cot1 DNA to the hybridization mixture. Efficient suppression can be confirmed by the apparent lack of painting of tandemly repetitive DNA blocks contained in the constitutive heterochromatin of the chromosomes (for example, 1q12, 9q12, 16q12, 19 cen) by both test and control genomic DNA in contrast to an intensive, apparently homogeneous painting (for quantitative criteria see below) of all euchromatic chromosome arms by the control genomic DNA.

Fluorescence background assessment. In order to select images with homogeneous and intense chromosome painting, the coefficient of variation of the fluorescence intensity of the painting by the control DNA should be lower than 20%. Exposure times of less than 10 s should be sufficient to obtain maximum values for chromosomal pixels of about one-half of the dynamic range of the CCD camera.

Fluorescence dynamic range. The dynamic range of the fluorescence signals is evaluated by the mode of the fluorescence intensity of the chromosome painting divided by the fluorescence intensity outside of the chromosomes. The quotients were in the range of 2–6. High values (>4.5) gave best results, whereas images with values lower than 3 were excluded.

Metaphase image homogeneity. In order to asses the homogeneity of the field, the gravity center of the mask of the DAPI-stained metaphase spread was compared with the intensity weighted gravity center of the FITC, TRITC, and the ratio images. A shift of the gravity centers of more than four pixels for the ratio image and ten pixels for the FITC and TRITC images (in one direction) indicate either heterogeneous field illumination or staining, respectively (see Figs. 6, 7). A shift of this extent is not compatible with quantitative evaluation.

Granularity of chromosome painting. Speckled painting of chromosomes leads to a high-frequency noise in the ratio profile. A parameter to describe the granularity was defined. A uniform linear filter (5 × 5) was applied to the FITC, TRITC, or ratio image (uniform image). For chromosomal pixels, the square of the difference between the original image and the uniform image was computed and then normalized by the original image (see Fig. 8). The granularity of the FITC image (typically 0.5) was often more pronounced than that of the TRITC image (0.3). Metaphase spreads that revealed values higher than 1 were excluded from the analysis. We observed a correlation of granularity with probe labeling and detection schemes. The chromosome painting signal was more homogeneous if the probes were labeled directly using fluorochrome conjugated nucleotides (e.g., fluorescein dUTP). With such probes, the granularity parameter was approximately 0.35. It increased to values of 0.5 if biotinylated probes were detected with one layer of avidin FITC, and it increased to values of 0.8 if a signal amplification procedure—e.g., with one layer of biotinylated antibodies and one layer with avidin FITC—was applied.

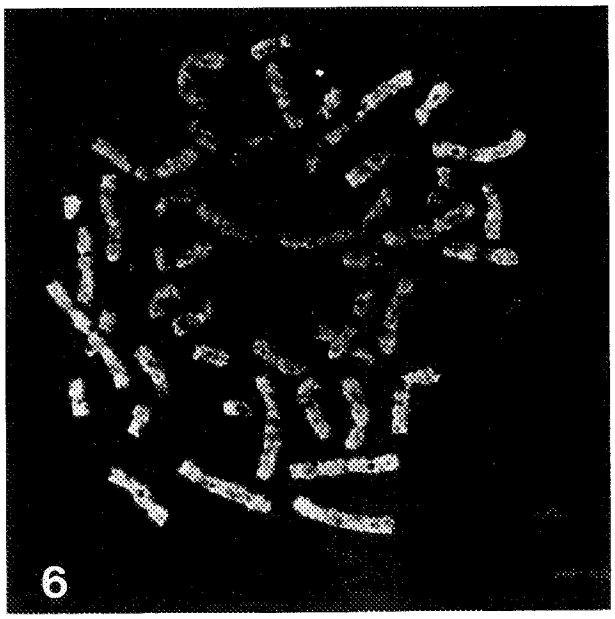

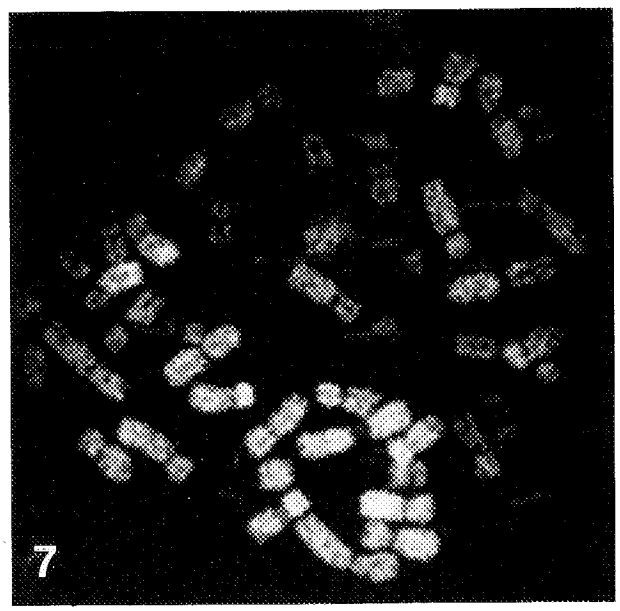

FIG. 6. Nonhomogeneous fluorescence ratio image. Due to heterogeneous illumination or fluorescence background staining, the fluorescence ratios vary from the periphery to the center of the field. The inhomogeneneity is detected by the gravity center shift parameter of the ratio image (value: horizontal shift = 0 pixels, vertical shift = 8 pixels). This image has to be excluded from the analysis.

FIG. 7. Nonhomogeneous FITC image. A group of chromosomes at the top of the image are noticeably more intensely labeled. This inhomogeneity is detected by the gravity center shift parameter of the FITC and ratio image (values for FITC, horizontal shift = 0 pixels, vertical shift = 16 pixels). This image has to be excluded from analysis.

Variability of ratio profiles of balanced chromosomal regions. The quality of a CGH experiment is re-

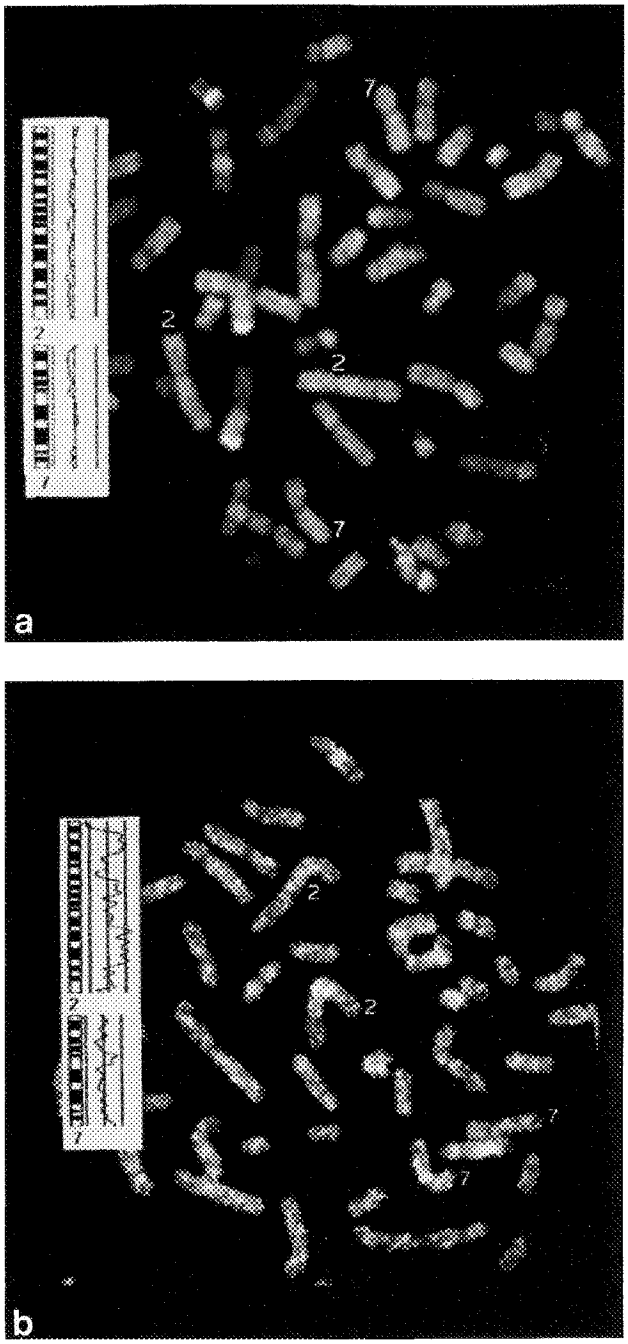

FIG. 8. FITC images of smooth and speckled chromosome painting patterns. **a:** Hybridization of DNA of an SCLC case (the same case as in Fig. 2). The average ratio profiles were smooth for five metaphase spreads with similar granularity (examples of chromosomes 2 and 7 are presented). The granularity parameter for this image equals 0.51. **b:** Hybridization of DNA of a medulloblastoma case. A significant high-frequency noise is present on the average ratio profile of seven metaphase spreads of similar granularity (examples of chromosomes 2 and 7 are presented). The granularity parameter for this image equals 1.9. Such a metaphase has to be excluded from the analysis.

flected by the variability of the average fluorescence ratio values for balanced chromosomal regions in the test genome. The following parameter was created with the assumption that the ratio distribution for balanced chromosomal regions can be extrapolated from the ratio distribution in the vicinity of the central value (the central value is the mode of the histogram in Fig. 5g). In a control CGH experiment (normal DNA vs. normal DNA), the average ratio values were assumed to follow a normal distribution. The standard deviation, coefficient of variation (SD/mean), and confidence intervals were calculated accordingly. The average ratio value distribution of a test CGH experiment is composed of values corresponding to balanced and unbalanced chromosome segments. An estimation of the spreading of the distribution (standard deviation and coefficient of variation) of the ratio values corresponding to the balanced status in test CGH experiments should describe the quality of the cytological preparation. For this purpose, the interval around the central value of the average ratio histogram containing 50% of the value was calculated. Assuming that 50% of the tumor genome is balanced and considering a normal density function, this interval is equal to $\times 0.67$ the standard deviation for the values corresponding to the balanced state. The standard deviation of the central value and the coefficient of variation of the balanced state ratio value (CVBS) is then computed and used to compare different experiments. The limit of the 95% confidence interval of the central value (central value $\pm$ 1.96 S.D.) can be calculated and could serve as the statistical thresholds (see below). The range of CVBS varied between 7% for optimal experiments and 25% for experiments with erratic profiles considered as noninformative.

Interphase Cytogenetics

A single-cell suspension of a human glioma (case 1 described in 20) was prepared as described (25); cells from acute myeloid leukemia (AML) patients (1) were prepared according to standard protocols. Dual-color FISH was performed with various DNA fragments cloned in plasmid, phage, cosmid, or yeast artificial chromosome (YAC) vectors. Alu-PCR amplification of YAC inserts and FISH was carried out as described (13,20). The hybridization efficiency of each clone was tested in nuclei of normal human lymphocyte preparations. Each of the clones showed two distinct signals in some 95% or more of these nuclei (data not shown). At least 100 nuclei from each tumor sample were evaluated. The following probes were used. The chromosomal map position is provided in parenthesis: YAC-clone HTY 3026 (5q13–14), HTY 3172 (7q36), HTY 3143 (9q21.1), HTY 3177 (9q13–21), HTY 3030 (16q23), HTY 3141 (17p13), and HTY 3147 (22q13). These clones were a generous gift of Helen Donis-Keller (St. Louis, MO). The clone HY 129 (21q22) was a generous gift of Drs. M.C. Poitier and M. Goedert (Cambridge, U.K.). The cosmid clone cos 29 (5q33) was provided by Greg Landes (Framingham, MA). The phage clones containing the RB1-gene were kindly provided by Thaddeus Dryja (Cambridge, MA; 27); three overlapping cosmids containing the p53 encoding genomic region (17p13) were kindly provided by Johannes Coy and Annemarie Poustka (Heidelberg); chromosome-specific

centromeric DNA probes of chromosomes 7, 8, and 12 cloned in plasmid vectors were kindly provided by Huntington Willard (Cleveland, OH).

RESULTS

The detection of chromosomal imbalances by the CGH ratio profile relies on the appropriate definition of thresholds defining the three intervals of normal (balanced), underrepresented, and overrepresented chromosomal material.

Fifty Percent Thresholds

The 50% threshold was designed for chromosomal imbalances present in 50% or more of the cells of a tumor sample (see above under Determination of the Thresholds). This threshold is only valid if there is a tight, linear correlation between the theoretical ratios and the ratios that can be obtained from a CGH experiment. If 50% of the cells carry a chromosomal imbalance, the theoretical ratios are 0.75 for a monosomy and 1.25 for a trisomy. These values were chosen as thresholds and tested with respect to their specificity and sensitivity regarding the detection of chromosomal imbalances in tumors. The ratio profiles of CGH experiments with normal control DNA vs. normal control DNA (for consideration of the gonosomes, the sex of both controls should be the same) served as a control experiment. In this case, the ratio profile is expected to stay within the interval defining the normal range with only small deviations from the central line as shown by the example presented in Figure 9.

The correlation between theoretical and experimental ratio values was assessed by a comparison of the expected ratio (deduced from the chromosomal copy number determined by interphase cytogenetics) with experimental CGH ratio values. For this comparison, an anaplastic astrocytoma was selected exhibiting multiple chromosomal gains and losses. The average ratio profile of this tumor is presented in Figure 10. Yeast artificial chromosome clones and chromosome-specific repetitive probes were hybridized to isolated nuclei of the tumor. The chromosomal position of these probes as well as the mean of the number of hybridization signals per cell are indicated in Figure 10. Plotting of these mean values vs. the ratio values of the corresponding chromosomal areas revealed a strong linear correlation ($r = 0.83$).

For two probes that map to 9q21.1 and 9q13–21 in the vicinity the heterochromatic block at 9q12, there was a notable deviation from the regression line: The enumeration of the interphase signal was consistent with three copies corresponding to the ratio values of distal 9q (and proximal 9p), whereas the targeted proximal 9q region exhibited even higher ratio values. These high ratios, however, have to be considered as artifacts derived from the heterochromatic region 9q12. Due to signal suppression by Cot1 DNA, segments such as 9q12 containing tandemly repetitive DNA show only residual staining (Fig. 11). Accordingly, ratio values obtained for such regions may be exceedingly high or low, although the region is present in balanced copy number. For this reason, the ratio values obtained for heterochromatic regions are generally neglected in CGH studies (9,10,19,20,22–24). Due to limitations of the spatial resolution of the CGH ratio profile along the idiogram, such erroneous ratio values may also affect regions in the immediate neighborhood, a problem that is observed in all chromosomal regions containing large, variable-sized heterochromatic blocks (for further considerations on spatial resolution, see Discussion).

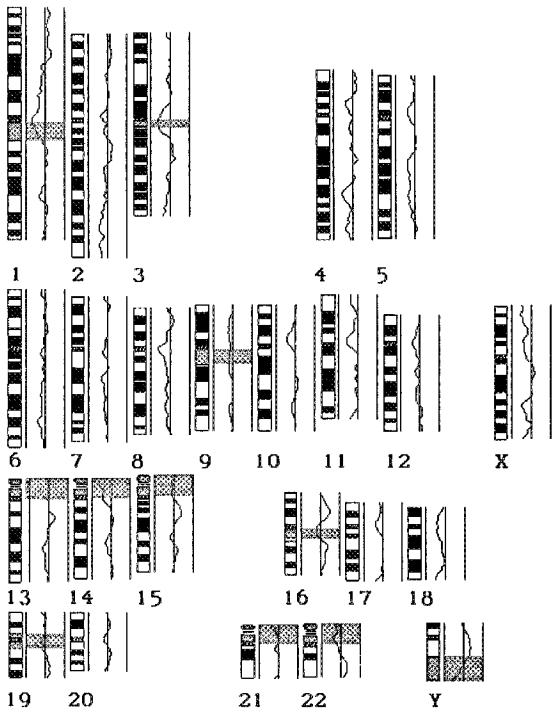

FIG. 9. The average ratio profile of a normal vs. normal CGH experiment (average of nine metaphases) displayed along the chromosome idiograms. The three vertical lines at the right side of each chromosome scheme indicate the two thresholds (50% thresholds displayed) flanking the central line (for definition, see text). Ratio values are in the normal range for all chromosomes. Except in the regions with high content of repetitive sequences (gray shaded boxes), the ratio value does not deviate significantly from the central line. The minimal average ratio value is found for chromosome 18 (0.93), and the maximum is found for chromosome 16 (1.04; calculated excluding the heterochromatin block).

In order to test the validity of the 50% threshold, we first analyzed the pseudodiploid cell line, ACHN, established from a single-cell clone of a cultured renal cell carcinoma (12). Average ratio profiles are shown in Figure 12 next to the chromosome idiograms. Applying the 50% thresholds, chromosomal gains were identified for 1q, 2, 7, 10q, 12, 16, and 17. Taking into account the near diploid state of the ACHN cell line, the profiles suggest a trisomic state of 1q, 2, 10q, 16, and 17 and a tetrasomy of 7 and 12. This is in full agreement with the results of chromosomal banding (12) and previous CGH experiments using chromosome mask measurements (3).

CGH analyses are often carried out with tumor material

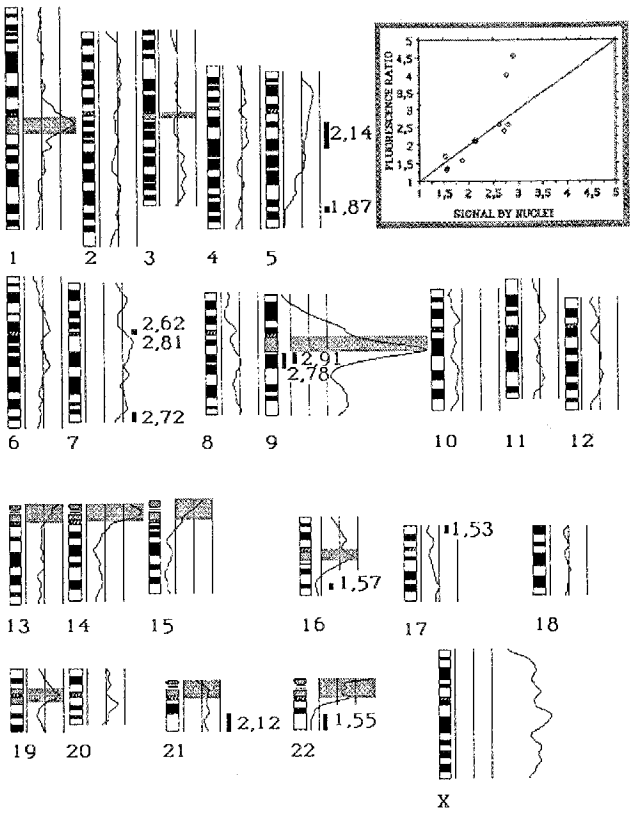

FIG. 10. Comparison of average ratio profiles with interphase cytogenetic analysis in an anaplastic astrocytoma (average of ten metaphases). Black bars indicate the mapping positions of yeast artificial chromosome (YAC) clones and alphoid DNA sequences (probes are listed in Materials and Methods). At the right of each bar, the average number of signals is given for 100 nuclei from an uncultured cell sample. The **inset** (top right) shows the average signal number for each probe according to the average fluorescence ratios calculated for the corresponding regions. The balanced state was assumed to correspond to the pseudodiploid state (regression value = 0.83; 50% thresholds displayed). For further explanations, see text.

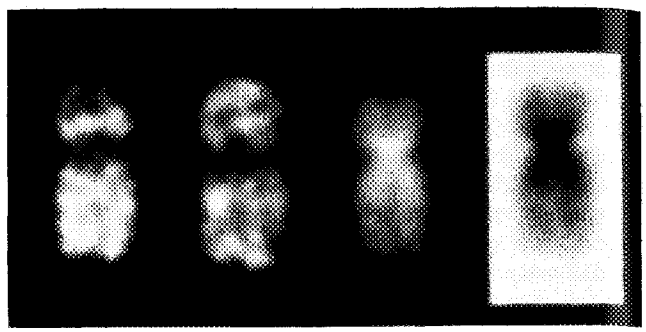

FIG. 11. FITC, TRITC, and DAPI images and inverse video DAPI image (left to right) of chromosome 9 (same case as Fig. 10). Only residual hybridization intensities are present on the 9p11–q12 region due to suppression of the hybridization of repeated sequences by the Cot 1 fraction of human DNA.

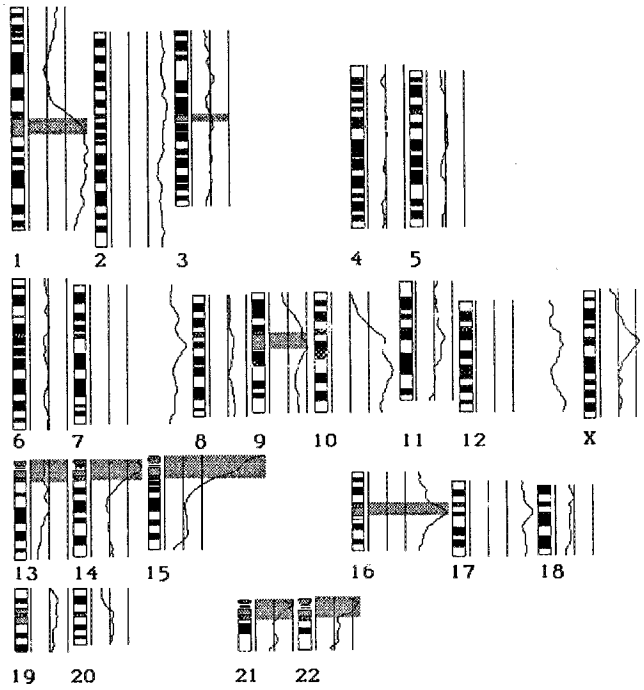

FIG. 12. The average ratio profile for the cell line ACHN (using nine metaphase spreads) displayed with 50% thresholds. All ratio values are outside the normal range. The chromosomes or chromosomal arms 1q, 2, 7, 10q, 12, 16, and 17 are consistent with the chromosomal imbalances previously described by banding analysis. In the gray-shaded regions, ratio values are not interpretable. These regions consist of clustered, repetitive DNA sequences that are partly suppressed within the probe sequences under the experimental conditions used.

containing several cell clones with different karyotypes. Because the thresholds of 0.75 and 1.25 correspond to the values that are expected for chromosomal imbalances present in one-half of the cells, it was important to examine the validity of the thresholds with test DNA from blood samples that contained certain clonal aberrations in a known proportion of the cells (interphase cytogenetics data).

As a test, in ten cases of nearly diploid acute myeloid leukemia, we compared the identification of chromosomal imbalances by CGH with the results of G-banding analysis and the frequency of certain clonal aberrations by interphase cytogenetics (1). Applying the 50% threshold, concordant results were obtained for all chromosomes (except chromosome 19) when the imbalances were present in more than 35% of the cell population (the only two examples with proportions $\leq$35% are shown in Fig. 13). Notably, the clonal representations observed by interphase cytogenetics allow a direct comparison with the CGH data, since both experiments were performed with aliquots from the same uncultured material. Accordingly, percentages of cells with chromosomal imbalances given below all refer to interphase cytogenetics data. In two cases, the ratio profiles for chromosome 19 displayed values outside of the normal range (subregions corresponding to the bands p13.3 and q13.3), although banding analyses indicated no abnormal-

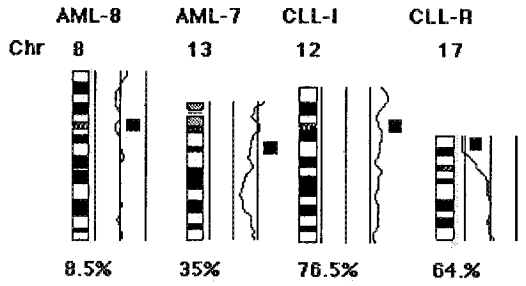

FIG. 13. Comparison of average ratio profiles of chromosomes from acute myeloid leukemia (AML) and chronic lymphoid leukemia (CLL) cases with interphase cytogenetic results. Black squares indicate the map positions of DNA probes used (probes are listed in Materials and Methods). Ratio values for chromosomal regions showing aberrations in 8.5% and 35.0% of the cells using interphase cytogenetics were within the normal range and cannot be detected using 50% thresholds. Aberrations present in higher percentages of the cells were clearly detectable, as the ratio values for these chromosomal subregions were outside the normal range.

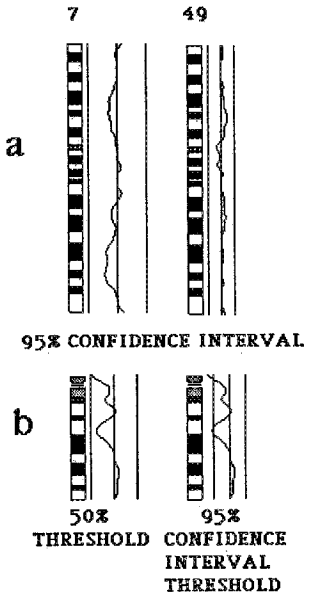

FIG. 14. Sensitivity of the 95% confidence interval. **a:** 95% Confidence interval for AML cases 7 and 49. The width of the interval can vary widely (exemplified for the chromosome 2) according to the variation of the ratio value for balanced chromosome as assessed by the coefficient of variation of the balanced state ratio value (CVBS; case 7, 16.55; case 49, 7.4; see also Table 1). **b:** A deletion involving the chromosomal band 13q14 was not detected with the 50% threshold but was detected with the 95% confidence interval, demonstrating the higher sensitivity of this threshold (in case of low CVBS). This deletion was independently found by interphase cytogenetics using the RB-1 probe located within 13q14.

ities. This unexpected variation of the ratio for chromosome 19 was associated with low suppression as assessed by the signal intensities on the heterochromatic blocks at 1q12, 9q12, and 16q12. Chromosome 19 is known to be highly enriched in small, interspersed repetitive elements (SINEs). Incomplete suppression of SINEs could result in ratio deviations due to polymorphisms of SINE sequences between test and control DNA rather than to changes of the chromosomal copy number.

In ten cases of chronic lymphocytic leukemias (CLL) exhibiting two normal copies for chromosome 19 by banding analysis, the chromosome 19 average ratio profiles were entirely in the normal range except for one case. In this case, the CGH ratio profile suggested an overrepresentation of the chromosome. Interestingly, the FITC and TRITC painting pattern showed an R-banding-like distribution (see Discussion).

For two cases of the CLL series, the copy number of the unbalanced chromosomal regions was determined by interphase cytogenetics (Fig. 13). In cases where a chromosomal imbalance was present in >50% of the cells (CLL-I and CLL-R), the average ratio profiles were clearly outside the normal range, whereas imbalances present in less than 50% of the cells (AML-7 and AML-8) resulted in average ratio values within the normal range.

Statistical Threshold

As an alternative to thresholds defined for the presence of a numerical aberration in a certain proportion of a cell clone (such as the 50% threshold), thresholds can also be defined by a 95% (central value ± 1.96 S.D.) or 99% confidence interval (central value ± 2.57 S.D.). Applying the 95% interval to the set of AML cases, the same chromosomal imbalances were found as with the 50% thresholds, i.e., aberrations in less than 35% of the cell population escaped detection. Figure 14 shows two examples illustrating the relationship of the width of the interval with the coefficient of variation of the balanced state value (CVBS). For comparison with the 50% threshold, multiplicative coefficients of the central value were calculated from the 95% and 99% confidence intervals (Table 1). With higher confidence intervals, the sensitivity to detection of imbalances decreases. Accordingly, with the 99% interval, several imbalances were missed within the AML cases (only four chromosomal imbalances were detected by CGH from a total of eight imbalances detected by G-banding). The 95% interval showed a sensitivity similar to the 50% thresholds; six out of eight aberrations were detected. The two chromosomal imbalances missed by the 95% confidence interval were confirmed by interphase cytogenetics to be present in 35% and 8.5% of the nuclei (Fig. 13). The minimal percentage of cells carrying an aberration, which can be detected with the 95% confidence interval, is clearly dependent on the quality of the preparation (i.e. the CVBS): the case carrying an aberration in 35% of the interphase nuclei (AML-7) has a high CVBS (16.55%); however, with low CVBS (9.3%, CLL-H), the 95% confidence interval proved to be more sensitive. For example, a deletion involving the chromosomal band 13q14 confirmed by interphase cytogenetics was found with the 95% confidence interval but was missed by the 50% threshold (Fig. 14).

Table 1
Multiplicative Coefficients Applied to the Central Value for 95% and 99% Confidence Interval Thresholds for the Ten AML Cases (in Each Case, Seven to Ten Metaphase Spreads Were Analyzed)[a]

	Multiplicative coefficient			
Case	95% Confidence interval		99% Confidence interval	
2	0.73	1.27	0.67	1.33
7	0.69	1.31	0.52	1.48
8	0.75	1.25	0.68	1.32
11	0.73	1.27	0.66	1.34
12	0.76	1.24	0.69	1.31
49	0.86	1.14	0.81	1.19
1071	0.67	1.33	0.58	1.42
1748	0.83	1.17	0.77	1.23
2388	0.78	1.22	0.70	1.30
F	0.72	1.28	0.66	1.34

[a]The sensitivity of the 99% interval is insufficient (see text). Note the important variation in width of the interval between cases (by example, cases 7 and 49). Note that the smallest interval is found for case 49. For considerations on the sensitivity in terms of percentage of cells carrying imbalances, see Discussion. For comparison, the multiplicative coefficient for the 50% threshold is 0.75 and 1.25.

Spatial Resolution

In order to assess the ability of the CGH method to physically map the borders of unbalanced regions, chromosomes with partial imbalances were considered. Within the series of test cell samples obtained from AML and CLL patients, there were six partial imbalances. In these cases, the chromosomal breakpoints, as determined by banding analyses, were in the following bands; 6q13, 6q25, 7q11.2, 7q22, 17p11, and 17p11.2. These breakpoints were compared to the position of the intersection of the ratio profile with a line placed in the middle between the central line and the 50% threshold line. Using the resulting intersection to delineate the borders of the deleted segments in the 400-band idiogram, we could map these borders to the same chromosomal bands as observed by banding analysis of tumor metaphase spreads. For further discussion of the spatial resolution, see below.

DISCUSSION

We have developed and tested a program for the quantitative evaluation of CGH experiments.

Descriptive and Exclusive Parameters

Objective parameters were defined to select images of reference metaphase spreads suitable for the calculation of fluorescence ratio profiles. Nonhomogeneous illumination of the optical field and fluorescent background staining resulted in regional variations of the fluorescence intensities and, thus, affected the precision of average ratio fluorescence profiles. Theoretically, taking the ratio should compensate for such nonuniform illumination or inhomogeneous background staining. However, experiments showed that only little variation of the illumination is tolerable. The inhomogeneity of the illumination and the immunological background can be controlled by gravity center shift parameters (see above under Metaphase Spread Homogeneity). In the present experiments, different filter sets were used for each fluorochrome. The following filter combination, as proposed by Dan Pinkel (University of California, San Francisco), should minimize the differences of illumination due to different wave lengths: three excitation band-pass filters mounted on a movable wheel, a fixed triple band-pass dichroic mirror, and a fixed triple band-pass emission filter (Chroma Technology Corp.). It should be emphasized that the granularity parameter as described above was found to be particularly useful in excluding metaphase spreads with speckled hybridization signals from further evaluation.

To estimate the overall quality of a CGH preparation, the coefficient of variation of the balanced state ratio value (CVBS) is very valuable. It allows objective assessment of the quality of the preparation. The accuracy with which chromosomal imbalances can be determined increases with decreasing CVBS. In preparations with a very small CVBS, the determination of imbalances should be possible even for subpopulations comprising <50% of the cells of a given test cell sample. CVBS provides a powerful tool for evaluating the effect of modifications in CGH protocols used in different laboratories.

Fluorescence Background Evaluation and Ratio Calculation

The determination of the fluorescence background staining is a critical step. Background fluorescence outside of the chromosome area results from the autofluorescence of the microscopic system and the glass slides and from the immunological background due to nonspecific binding of fluorescent reagents. Calculations of the fluorescence ratios performed after subtraction of the fluorescence intensity outside of the chromosome area for each fluorochrome lead to fluorescence ratios for chromosomal imbalances that are significantly closer to the value of 1.0 than the ratio that would be predicted from theoretical considerations. For example, the expected ratio value for a chromosome present in three copies in a pseudodiploid cell sample is 1.5. Figure 15 illustrates the effect of different background values on the ratio dynamic range: The background calculation described in Materials and Methods (ratio 1, Fig. 15) leads to a ratio close to the theoretically expected value, i.e., 1.5 for a trisomic segment or 0.5 for a monosomic segment. Subtraction solely of the background fluorescence measured outside of the chromosome area (ratio 2, Fig. 15) leads to ratio values closer to the central line. Without any background subtraction (ratio 3, Fig. 15), the fluorescence ratios were found closest to this line.

The fluorescence intensities measured along a given chromosome (except for heterochromatic blocks) is, in general, a summation of 1) specific fluorescence derived from hybridized probe fragments that are unique to this chromosome; 2) fluorescence from interspersed, repetitive sequences contained in the test and control DNA that

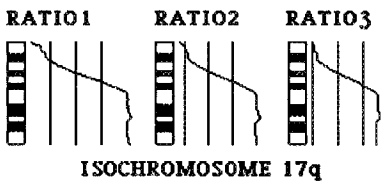

FIG. 15. Effect of the type of fluorescence background subtraction on the dynamic range of the ratio. Ratio 1: The fluorescence intensity of the whole image (excluding nuclei area) is used for the calculation of the fluorescence background. Ratio 2: The fluorescence intensity outside the metaphase area is used to estimate the fluorescence background. Ratio 3: No background correction. Ratio 1 results in ratio values closest to the theoretical values for monosomy (0.5), trisomy (1.5), etc. The left and right lines correspond to the values 0.75 and 1.25, respectively.

can become a major source of background fluorescence within a chromosome mask in case of suboptimal suppression conditions; and 3) background fluorescence due to nonspecific binding of labeled probe and detection reagents. Ideally, the second and third of these fluorescence sources should be subtracted from the first fluorescence source for optimal fluorescence ratio dynamic. In practice, it may be difficult to fulfill this requirement for CGH experiments. Although, in most FISH experiments, the background to be subtracted can be measured on nonlabeled chromosomes (3), such a procedure is not possible in CGH preparations. Therefore, the background to be subtracted must be estimated in a different way. In this study, the mean fluorescence of the image excluding cell nuclei was subtracted as background (ratio 1, Fig. 15). This value roughly equals the subtraction of 20% of the fluorescence intensity of the chromosomes. The described background correction was extensively tested in some 140 CGH experiments performed in two different laboratories including 15 different types of malignant tumors. When compared to several other procedures of background correction (e.g., 8), the background correction described here produced more stable fluorescence ratio profiles in our hands for balanced chromosome regions and produced fluorescence ratio dynamics that are closer to the theoretical values for near diploid cell samples (monosomy, 0.5; disomy, 1; trisomy, 1.5, and so forth).

Thresholds

A series of ten AML cases with fully analyzed karyotypes was used to test the program as well as the definition of the normal range between the 50% thresholds. Except for aberrations present in only a low percentage of the tumor nuclei, as expected from the definition of these thresholds, CGH results were in full agreement with the data from banding analysis (Fig. 13). In our experience, this threshold is very specific but of limited sensitivity, since only aberrations present in at least 50% of the cell population can be found. For chromosome 19, fluorescence values outside of the normal range have to be interpreted with caution in experiments with insufficient suppression hybridization conditions (see Results). Such an insufficient suppression could also result in chromosome painting revealing an R-banding-like pattern, since the most frequent interspersed, repetitive sequence elements, the Alu elements, are predominantly located within chromosomal R-bands (11,15).

The 50% thresholds, designed for near diploid cells, have a lower sensitivity with respect to the detection of genetic imbalances when applied to cell populations in which near triploid or tetraploid cells are predominant. For such cell populations, the theoretical ratio for a loss or a gain of one copy of a given chromosome in 50% of the cells is closer to the central value than in the case of near diploid cells. For example, in the case of near triploid cells, the values are 0.84 for the loss of one chromosome copy (instead of 0.75 for near diploid cells) and 1.17 for a gain of one copy (instead of 1.25). The most straightforward solution to defining the proper theoretical threshold is to measure the ploidy of the tumor sample by independent methods. Based on this evaluation, an appropriate threshold can be defined more accurately (see Materials and Methods). Such approaches are presently being tested.

Alternative thresholds designed on the basis of the statistical distribution of the average ratio value for balanced chromosomal regions in the tumor sample were also applied. The 95% confidence interval of the central value provided efficient thresholds (see above under Determination of the Thresholds) that proved to be a good compromise between sensitivity and specificity in our experiments. Using appropriate experimental conditions (CVBS lower than about 13%), the 95% confidence interval threshold was found to be more sensitive than the 50% threshold. Table 1 shows the low and high limit of the 95% confidence interval for the ten AML cases. The smallest interval was found for case 49 (see Table 1; 0.86–1.14), which did not reveal any imbalances. This interval theoretically excluded subclones with trisomies or monosomies comprising a fraction of more than 28% of the cell sample ($0.28 \times 1.5 + 0.72 \times 1 = 1.14$). In conclusion, we are confident that, in CGH experiments with low CVBS, a monosomy or trisomy present in even a lower percentage than 50% of the cell population can be detected using the statistical threshold. This statement is currently being tested.

Spatial Resolution

The boundaries of partial chromosomal imbalances mapped by CGH analysis were compared in six leukemia cases with the breakpoints determined by chromosomal banding analysis. In all cases, the band assignments of the boundaries were consistent with the breakpoints defined by conventional tumor cytogenetics.

For further refinement of chromosomal map positions of the boundaries of the imbalanced regions, two main problems must be solved. 1) The linear stretching of the individual ratio profiles to a predefined length should take into account regional differences in the condensation of chromosomes of different length. For small, interstitial deletions and partial trisomies, a procedure of dif-

ferential stretching of the ratio profile (from the initial length to the predefined length) according to landmark bands or appropriate chromosomal bar codes (14) should compensate for a nonlinear condensation of the chromosomes. 2) The second major limitation is related to the comparison of the ratio profile and the chromosome idiograms. There are no reports available in the literature that specifically describe the approaches used for the positioning of chromosomal bands in the 1985 ISCN idiograms (4,16). Thus, the chromosomal position defined after CGH might not be directly comparable to the ISCN idiograms. New chromosome idiograms inferred from DAPI fluorescence intensity profiles or other chromosome banding procedures applicable to CGH experiments may help to solve this problem (4). The smallest deleted segments that we could detect so far by CGH were in the order of 10 Mbp. A case in point is the deletion of band 17p13 in a CLL case, although some deletions on 13q involving the Rb gene may be even smaller (see Fig. 14b).

Number of Metaphases

The optimal number of reference metaphases that need to be evaluated for reliable CGH analyses is not clear at present. For an optimal spatial resolution, metaphase spreads should be selected according to the following features (described in Materials and Methods): 1) elongated chromosomes with a similar degree of condensation as assessed by the chromosome length parameter and 2) a smooth painting pattern as assessed by the granularity parameter. For a maximal accuracy of relative copy number assessments, low variability of the fluorescence ratio values (described by the CVBS of individual metaphase spreads) as well as high fluorescence dynamics are required. In our hands, evaluation of five to 12 metaphase spreads (generally ten) fitting these requirements gave acceptable results.

More than 140 cases of different tumor entities were investigated by CGH in our laboratories (1,3,19,20,22–24, unpublished data) using the program described here. In all of the published work referenced above, the delineation of chromosomal imbalances was based on the analysis of five to ten metaphase spreads using a 50% threshold. For most of the solid tumor specimens investigated by CGH, data from chromosome banding analyses were lacking. Furthermore, for hematological malignancies and some solid tumors, the results of banding analyses showed differences compared with CGH data. These conflicting data indicate that clones that are predominant in cultured cell samples may represent only a minor subclone in vivo (1,20). In the AML samples used for this study, interphase cytogenetics revealed the same clonal frequencies of chromosomal imbalances in nuclei of uncultured and cultured samples (Bentz et al., in preparation). In many cases, the origin of a previously unknown amplification could be mapped by CGH including a series of malignant gliomas, small-cell lung carcinomas, and breast cancers (9,19,20). Consensus regions for partial gains and losses could also be mapped in these series providing a starting point for the positional cloning of genes whose overrepresentation or underrepresentation plays a role in tumor initiation, progression, and the formation of metastatic sites (2). Without quantitative evaluation applying the program presented here, the smallest deletions would have escaped detection in at least some of the cases studied in our laboratories.

ACKNOWLEDGMENTS

We thank Barbara Schütz, Heidi Holtgreve-Grez, Brigitte Schoell, and Marie-Christine Meffert for excellent experimental work. Hartmut Döhner (Heidelberg) is gratefully acknowledged for providing the cytogenetic data of leukemia cases. We thank Gyula Kovacs (Heidelberg) for the gift of DNA from the ACHA cell line. Johannes Coy and Annemarie Poustka (Heidelberg), Helen Donis-Keller (St. Louis), Thaddeus Dryja (Cambridge, U.K.), Greg Landes (Framingham, MA), M.C. Poitier and M. Goedert (Cambridge, MA), and Huntington Willard (Cleveland) kindly provided DNA probes.

LITERATURE CITED

1. Bentz M, Huck K, du Manoir S, Joos S, Schütz B, Döhner H, Lichter P: Identification of previously undetected chromosomal abnormalities in leukemias by comparative genomic hybridization. Blood 82(Suppl 1):122, 1993 (abstract).
2. Birrer M, Brown PH: Application of molecular genetics to the early diagnosis and screening of lung cancer. Cancer Res 52:2658s–2664s, 1992.
3. du Manoir S, Speicher MR, Joos S, Schröck E, Popp S, Döhner H, Kovacs G, Robert-Nicoud M, Lichter P, Cremer T: Detection of complete and partial chromosome gain and losses by comparative genomic in situ hybridization. Hum Genet 90:590–610, 1993.
4. Francke U: Digitized and differentially shaded human chromosome for genomic applications. Cytogenet Cell Genet 65:206–219, 1994.
5. Hilditch CJ: Linear skeletons from square cupboards. In: Machine Intelligence 4, Melzer B, Michie D (eds). Edinburgh University Press, Edinburgh, 1969, pp 403–420.
6. ISCN: In: An international system for cytogenetic nomenclature, Harnden DG Klinger HP (eds). S Karger AG, New York, 1985.
7. Joos S, Scherthan H, Speicher MR, Schlegel J, Cremer T, Lichter P: Detection of amplified genomic sequences by reverse chromosome painting using genomic tumor DNA as probe. Hum Genet 90:584–589, 1993.
8. Kallioniemi A, Kallioniemi OP, Sudar D, Rutovitz D, Gray JW, Waldman F, Pinkel D: Comparative genomic hybridization for molecular cytogenetic analysis of solid tumors. Science 258:818–821, 1992.
9. Kallioniemi A, Kallioniemi OP, Piper J, Tanner M, Stokke T, Chen L, Smith HS, Sudar D, Pinkel D, Gray JW, Waldman F: Detection and mapping of amplified DNA sequences in breast cancer by comparative genomic hybridization. Proc Natl Acad Sci USA 91:2156–2160, 1994.
10. Kallioniemi OP, Kallioniemi A, Sudar D, Rutovitz D, Gray JW, Waldman F, Pinkel D: Comparative genomic hybridization: A rapid new method for detecting and mapping DNA amplification in tumors. Sem Cancer Biol 4:41–46, 1993.
11. Korenberg JR, Rykowski MC: Human genome organization: Alu, lines, and the molecular structure of metaphase chromosome bands. Cell 53:391–400, 1988.
12. Kovacs G, Fuzesi L, Emanuel A, Kung H: Cytogenetics of papillary cell tumors. Genes Chrom Cancer 3:249–255, 1991.
13. Lengauer C, Green ED, Cremer T: Fluorescence in situ hybridization of YAC clones after Alu-PCR amplification. Genomics 13:826–828, 1992.
14. Lengauer C, Speicher MR, Popp S, Jauch A, Taniwaki M, Nagaraja R, Riethman HC, Donis-Keller H, D'Urso M, Schlessinger D, Cremer T: Chromosomal bar codes produced by multicolor fluorescence in

situ hybridization with multiple YAC clones and whole chromosome painting probes. Hum Mol Genet 2:505–512, 1993.
15. Manuelidis L, Ward DC: Chromosomal and nuclear distribution of the Hind III 1.9 kb human DNA repeat segment. Chromosoma 91: 28–38, 1984.
16. Mark HFL, Parmenter M, Campbell W, Mark R, Zolnierz JK, Dunwoodie D, Hann E, Airall E, Santoro K, Mark Y: A novel, convenient, and inexpensive approach for deriving ISCN(1985) relative lengths: Validation by a morphometric study of 100 karyotyped metaphase cells. Cytogenet Cell Genet 62:13–18, 1993.
17. Morton NE: Parameters of the human genome. Proc Natl Acad Sci USA 88:7474–7476, 1991.
18. Piper J, Granum E: On fully automated feature measurement for banded chromosome classification. Cytometry 10:242–255, 1989.
19. Ried T, Petersen I, Holtgreve-Grez H, Speicher MR, Schröck E, du Manoir S, Cremer T: Mapping of multiple DNA gains and losses in primary small cell lung carcinomas by comparative genomic hybridization. Cancer Res 54:1801–1806, 1994.
20. Schröck E, Thiel G, Lozanova T, du Manoir S, Meffert MC, Jauch A, Speicher MR, Nürnberg P, Vogel S, Jänisch W, Donis-Keller H, Ried T, Witkowski R, Cremer T: Comparative genomic hybridization of human malignant gliomas reveals multiple amplification sites and non-random chromosomal gains and losses. Am J Pathol 144:1203–1218, 1994.
21. Smith TG Jr, Marks WB, Lange GD, Sheriff WH Jr, Neale EA: Edge detection in images using Marr-Hildreth filtering techniques. J Neurosci Methods 26:75–81, 1988.
22. Speicher MR, du Manoir S, Schröck E, Holtgreve-Grez H, Schoell B, Lengauer C, Cremer T, Ried T: Molecular cytogenetic analysis of formalin fixed, paraffin embedded solid tumors by comparative genomic hybridization after universal DNA amplification. Hum Mol Genet 2:1907–1914, 1993.
23. Speicher MR, Prescher G, du Manoir S, Jauch A, Hormstemke B, Bornfeld N, Becher R, Cremer T: Chromosomal gains and losses in uveal melanomas detected by comparative genomic hybridization. Cancer Res 54: 3817–3823, 1994.
24. Speicher MR, Schoell B, du Manoir S, Ried T, Störkel S, Kovacs A, Cremer T, Kovacs G: Specific loss of chromosomes 1, 2, 6, 10, 13, 17, and 21 in chromophobe renal cell carcinomas revealed by comparative genomic hybridization. Am J Pathol 145:356–364, 1994.
25. Thiel G, Lozanova T, Kintzel D, Nisch G, Martin H, Vorpahl K, Witkowski R: Karyotypes of 90 human gliomas. Cancer Genet Cytogenet 58:109–120, 1994.
26. Waggoner A, Debasio R, Conrad P, Bright GR, Ernst L, Ryan K, Nederlof M, Taylor D: Multiple spectral parameter imaging. Methods Cell Biol 30:449–478, 1989.
27. Wiggs J, Nordenskjöld M, Yandell D, Rapaport J, Grondin V, Janson M, Werelius B, Petersen R, Craft A, Riedel K, Liberfard R, Walton D, Wilson W, Dryja TP: Prediction of the risk of hereditary retinoblastoma, using DNA polymorphisms within the retinoblastoma gene. N Engl J Med 318:151–157, 1988.